JOURNAL OF CATALYSIS 10, 377–390 (1968)

Studies on Pore Systems in Catalysts

XIII. Pore Distributions from the Desorption Branch of a Nitrogen Sorption Isotherm in the Case of Cylindrical Pores

B. Applications

J. C. P. BROEKHOFF AND J. H. DE BOER

From the Department of Chemical Technology, Technological University of Delft, The Netherlands

Received November 15, 1967; revised January 10, 1968

Calculations of cylindrical pore distributions from the desorption branch of nitrogen sorption isotherms may be performed with the aid of a corrected form of the Kelvin equation. Quantitative evaluation of the influence of adsorption forces on capillary evaporation from pores in oxydic adsorbents shows that the application of the classical uncorrected Kelvin equation to pore-size determinations from sorption isotherms leads to values for the pore radius which are too small.

The theoretical width of the hysteresis loop for open cylinders is determined as a function of relative pressure. The results of this calculation are applied to the analysis of pore shape from the width of the hysteresis loop.

A comparison is made between the results of pore-size distribution calculations from the desorption branch and those from the adsorption branch as calculated according to a method discussed in a preceding part of this series. In appropriate cases, there is a fair agreement between both methods.

I. INTRODUCTION

In the preceding articles IX (*1*) and XII (*2*) of this series the evaporation of capillary-condensed liquid from a cylindrical pore was studied on a theoretical basis. It was shown that, according to the refined model of capillary condensation and evaporation presented in this series, the emptying of a cylindrical pore of radius r occurs at a pressure p_D, determined by the relation

$$r - t_e = \frac{2\gamma V_m}{RT \ln(p_0/p_D)} + \frac{\int_{t_e}^{r} 2F(t)(r - t)\, dt}{(r - t_e)RT \ln(p_0/p_D)} \quad (1)$$

where t_e represents the equilibrium thickness of the adsorbed layer in a pore of radius r at a relative pressure p_D/p_0; γ, the surface tension of the liquid–vapor interface; V_m, the molar volume of the liquid; and $F(t)$, a function representing the difference in intrinsic thermodynamic potential between the bulk liquid and an adsorbed phase of thickness t. The equilibrium thickness t_e, because of the curvature of the liquid–vapor interface of the adsorbed layer, was shown before to be different from the t value corresponding to a noncurved interface at the same relative pressure and temperature, and to be given by the solution of the equation [see Eq. (13) of Part IX]

$$RT \ln(p_0/p_D) - F(t_e) = \gamma V_m/(r - t_e) \quad (2)$$

The exact status of $F(t)$ may be clarified by the consideration that essentially $F(t)$ is the difference between the differential change in free enthalpy of the system at constant temperature and pressure upon adding dN moles of bulk liquid to the system *at infinite distance* [Eq. (11) of Part IX] and upon adding dN moles of condensed phase to the system in such a way that these dN moles will be situated *at a distance* t *from the solid*

pore wall, viz., adding dN moles of condensed phase to an adsorbed film of thickness t.

For a noncurved solid surface, $F(t)$ is entirely determined by the universal t curve of multimolecular adsorption, which is equal to the value of $RT \ln(p_0/p_D)$ corresponding to a thickness t of the adsorbed layer [see Part IX of this series (*1*)]. In a cylindrical pore, as a first approximation, it may be assumed that $F(t)$ is largely determined by the distance t to the pore wall and that the influence of the curvature of the pore wall on $F(t)$ may be neglected. Although there is no experimental evidence for the accuracy of this approximation (as there is hardly any experimental work available on the state of capillary-condensed liquid in not very wide pores) the results of the actual calculations of pore distributions, as presented in Part X of this series (*2*), suggest that the just-mentioned approximation may lead to satisfactory results in practice as long as no "sub-micropores," viz., pores with radii smaller than, say, 10 to 15 Å, are present.*

For wider pores actual deviations from the values predicted by this approximation may be largest in magnitude for capillary-condensed liquid present in or near the center of the pore, as capillary-condensed liquid present in these positions is surrounded symmetrically by solid pore walls at all sides. This last consideration may cast some doubt on the practical validity of evaluation of Eq. (1) with the aid of expressions for $F(t)$ based on the t curve of multimolecular adsorption. Fortunately, the actual correction term to the Kelvin equation involved, the second term at the right side of Eq. (1), contains as the integrand not $F(t)$, but rather $(r - t)F(t)$. It is seen that the integrand vanishes at the center of the pore, where the exact status of $F(t)$ is uncertain, and is very small near the center of the pore, thus hardly contributing to the numerical value of the correction term involved. Both the terms $F(t)$ and $(r - t)$ increase with decreasing t, so the largest contribution to the correction term is obtained from capillary-condensed liquid near the walls of the pore, where it is to be expected that an expression for $F(t)$, obtained from the universal t curve of multimolecular adsorption, is sufficiently accurate for not too narrow cylindrical pores.

Thus, we may assume the use of values for $F(t)$ from the t curve of multimolecular adsorption for the evaluation of (1) and (2), to be justifiable at least in first approximation.

II. Numerical Evaluation of Equations Governing Evaporation from Cylindrical Pores

As was stated in Part X of this series (*2*), at the normal boiling point of nitrogen the t curve of multimolecular nitrogen adsorption is described with sufficient accuracy by means of

$$\log\left(\frac{p_0}{p}\right) = \frac{13.99}{t^2} - 0.034 \qquad \text{for } t < 10 \text{ Å} \quad (3a)$$

and

$$\log\left(\frac{p_0}{p}\right) = \frac{16.11}{t^2} - 0.1682 \exp(-0.1137t) \qquad \text{for } t > 5.5 \text{ Å} \quad (3b)$$

Consequently, $F(t)$ may be approximated by

$$\frac{F(t)}{2.303RT} = \frac{13.99}{t^2} - 0.034 \qquad \text{for } t < 10 \text{ Å} \quad (4a)$$

and

$$\frac{F(t)}{2.303RT} = \frac{16.11}{t^2} - 0.1682 \exp(-0.1137t) \qquad \text{for } t > 5.5 \text{ Å} \quad (4b)$$

For the surface tension and molar volume of liquid nitrogen at its normal boiling point the following values were adopted:

$$\gamma = 8.72 \text{ dynes/cm}$$
$$V_m = 34.68 \text{ cm}^3\text{/mole}$$

With the aid of (3) and (4) the integral factor

* Other authors, e.g., Dubinin (*3*), call these pores "micropores" and use the word "intermediate pores" for those which we call micropores, viz., pores <500 Å.

$$\int_{t_e}^{r} (r - t)F(t)\,dt$$

may be calculated to be equal to

$$\int_{t_e}^{r} F(t)(r - t)\,dt = 2.303RT\left\{13.99\left[\frac{r}{t_e} - 1 - \ln\left(\frac{r}{t_e}\right)\right] - 0.017(r - t_e)^2\right\} \quad (5a)$$

or

$$\int_{t_e}^{r} F(t)(r - t)\,dt = 2.303RT\left\{16.11\left[\frac{r}{t_e} - 1 - \ln\left(\frac{r}{t_e}\right)\right] - 1.482\exp(-0.1137t_e)[r - t_e - 8.795] - 13.03\exp(-0.1137r)\right\} \quad (5b)$$

respectively, where t_e is the equilibrium thickness.

With the aid of these expressions, at the normal boiling point of liquid nitrogen, the corrected Kelvin equation for the nitrogen evaporation from cylindrical pores present in inorganic oxides and related substances, is calculated to be equal to

$$r - t_e = \frac{4.05}{\log(p_0/p_D)} + \frac{27.98\{(r/t_e) - 1 - \ln(r/t_e)\} - 0.034(r - t_e)^2}{(r - t_e)\log(p_0/p_D)} \quad (6a)$$

and

$$r - t_e = \frac{4.05}{\log(p_0 p_D)} + \frac{32.22\{(r/t_e) - 1 - \ln(r/t_e)\}}{(r - t_e)\log(p_0/p_D)} - \frac{2.964\exp(-0.1137t_e)[r - t_e - 8.795]}{(r - t_e)\log(p_0/p_D)} - \frac{26.06\exp(-0.1137r)}{(r - t_e)\log(p_0/p_D)} \quad (6b)$$

respectively.

For pores of a radius not exceeding 10 Å, Eq. (6a) would be the appropriate expression for the Kelvin equation (but the concept of capillary condensation and other related concepts are very doubtful for pores smaller than 10 Å), whereas for wider pores, where t_e generally exceeds 5.5 Å, Eq. (6b) is a more accurate expression. Thus, in spite of the relative complexity of (6b), this last equation is the one indicated for practical use in the calculation of pore distributions. Expression (6) is a relation between r, t_e, and p_0/p_D, and so this relation may not be solved directly for r as a function of p_D.

A second relation between the three parameters mentioned, may be obtained from Eq. (2) on substituting the appropriate expressions for $F(t)$; γ, and V_m. This leads to the alternative expressions already discussed extensively in Part X of this series:

$$\log\left(\frac{p_0}{p_D}\right) = \frac{13.99}{t_e^2} - 0.034 + \frac{2.02^5}{(r - t_e)} \quad (7a)$$

and

$$\log\left(\frac{p_0}{p_D}\right) = \frac{16.11}{t_e^2} - 0.1682\exp(-01137t_e) + \frac{2.02^5}{(r - t_e)} \quad (7b)$$

respectively.

The most convenient way of solving (6) and (7) simultaneously is to substitute (5) into (4) and solve for t_e, for a larger number of given values of r. From the values of t_e belonging to specified values of r, the corresponding relative pressures p_D/p_0 may be calculated from (7). As it is in general desired to obtain the value of r corresponding to a certain relative pressure p/p_0, this value has to be calculated from a table of p/p_0 as a function of r by interpolation. In order to ensure sufficient accuracy, it is necessary to calculate the relative pressure of desorption for a large number of r values over the whole range of relative pressures involved. Up to radii of 20 Å, the results obtained from (6a) and (7a) are quite consistent with those obtained from (6b) and (7b), whereas for larger pore radii (6b) and (7b) should always by used.

Actually, the application of (6a) and (7a) over the whole relative pressure range would lead to the conclusion that even at saturation only pores with a radius below a certain critical radius, approximately 190 Å, would remain filled with capillary condensate, which is highly improbable on

physical grounds and contrary to the seemingly asymptotic behavior of many sorption isotherms near saturation. The anomalous behavior of the solutions of (6a) and (7a) is caused by the finite number of layers adsorbed at saturation, that would follow from adsorption equations of the Harkins-Jura type (*4*), such as (3a), together with the supposition of continuity in the state of the capillary-condensed liquid upon increasing distance from the solid adsorbent wall. As will be shown in another paper in this series, the formula derived by Derjaguin (*5*) for capillary evaporation (Derjaguin assumed slit-shaped pores, but the pore model is not essential for the argument), does not possess the property of a critical radius when used in conjunction with an adsorption equation of the Harkins-Jura type, as the treatment of Derjaguin implicitly assumes a sort of discontinuous transition between the adsorbed layer of saturation thickness and bulk condensed liquid. In the present treatment the continuity between adsorbed and capillary-condensed phase has been one of our fundamental starting points.

For the adsorption of nitrogen at nonporous adsorbents there are no indications of a finite number of layers adsorbed at saturation. It must be borne in mind, however, that the problem of a finite number of layers and the problem of contact angle, may become important in studying the adsorption of other adsorbates, such as, e.g., water vapor in certain adsorbents, such as porous glass or porous carbon blacks.

The results of the calculations of the pore radii corresponding to certain relative pressure values p_D/p_0, are gathered in Table 1. For comparison, the radii corresponding to the uncorrected Kelvin equation,

$$r - t_a = \frac{2\gamma V_m}{RT \ln(p_0 p_D)} \qquad (8)$$

where t_a is the uncorrected value for the thickness of the adsorbed layer at the relative pressure p_D/p_0, which may be taken directly from the t curve of multimolecular adsorption, are included in Table 1.

III. Analysis of Hysteresis Loop Width for Cylindrical Pore Model—Problem of Sorption Hysteresis Inception

In the classical conception for an ideal cylindrical pores, open at both ends, the relative pressure of capillary condensation during adsorption, p_A, is connected with the relative pressure of capillary evaporation by (*6*)

$$\frac{\ln(p_D/p_0)}{\ln(p_A/p_0)} = \frac{2(r - t_a)}{(r - t_d)} \qquad (9)$$

which for large values of r reduces approximately to

$$p_D/p_0 = (p_A/p_0)^2 \qquad (10)$$

In the classical conception (9) would strictly hold for ideal open cylinders, provided the radii of the pores are all equal. It may be easily proved that the existence of a distribution of pore radii leads to a narrower hysteresis loop than would be predicted from (9), this relative narrowing being most pronounced at the lower relative pressure side of the hysteresis loop and vanishing at the higher closing point of the hysteresis loop, provided all pores in the porous substance have the same pore shape.

In the present treatment the desorption is governed by the modified Kelvin equation (1), while the adsorption branch is governed by a relation of a different type for the stability of the adsorption branch [Eq. (13) of Part IX of this series], so no simple relation analogous to (10) exists any more. It is, however, quite easy to calculate the width of the hysteresis loop from Table 3 of Part X and from Table 1 of the present treatment. In Table 2 the results of these calculations are reproduced. Instead of

$$\frac{(p_D/p_0)}{(p_A/p_0)}$$

the difference $(p_A/p_0) - (p_D/p_0)$ as a function of, for example, (p_A/p_0) is a measure of the width of the hysteresis loop, which is easier to handle, since the actual width of the hysteresis loop from measured isotherms as a function of (p_A/p_0) may be

TABLE 1
RELATIVE PRESSURES AT WHICH COMPLETE EMPTYING SHOULD TAKE PLACE WITH THE CORRESPONDING RADII (IN Å) IN CYLINDRICAL PORES

p/p_0	Radius of pores, as calculated from Eq. (6)	Radius of pores, as calculated from Eq. (8)
0.9975	4060	3844
0.9925	1415	1307
0.9875	876.0	792.8
0.9825	640.1	569.8
0.9775	507.0	444.7
0.9725	420.9	364.5
0.9675	360.6	308.9
0.9625	315.7	268.1
0.9575	281.0	237.0
0.9525	253.2	212.4
0.9475	230.6	192.5
0.9425	211.6	176.1
0.9375	195.6	162.3
0.9325	181.9	150.6
0.9275	170.0	140.5
0.9225	159.6	131.6
0.9175	150.3	123.8
0.9125	142.1	117.0
0.9075	134.8	110.8
0.9025	128.2	105.3
0.89	114.2	93.62
0.87	97.29	79.57
0.85	84.77	69.20
0.83	75.12	61.22
0.81	67.45	54.88
0.79	61.21	49.65
0.77	56.02	45.38
0.75	51.64	41.76
0.73	47.89	38.66
0.71	44.63	35.95
0.69	41.78	33.57

read directly from a graphical representation of the isotherms.

It must be realized, however, that the significance of the calculated width of the hysteresis loop is very doubtful when the relative pressure p_D/p_0 corresponding to a certain relative pressure p_A/p_0, reaches a value lower than 0.40. It is a well-known

TABLE 1 (*Continued*)

p/p_0	Radius of pores, as calculated from Eq. (6)	Radius of pores, as calculated from Eq. (8)
0.67	39.25	31.47
0.65	37.00	29.58
0.63	34.98	27.88
0.61	33.15	26.35
0.59	31.48	24.95
0.57	29.96	23.67
0.55	28.56	22.49
0.53	27.26	21.39
0.51	26.06	20.39
0.49	24.94	19.44
0.47	23.89	18.56
0.45	22.90	17.73
0.43	21.97	16.95
0.41	21.09	16.21
0.39	20.26	15.51
0.37	19.46	14.85
0.35	18.70	14.22
0.33	17.97	13.61
0.31	17.27	13.03
0.29	16.59	12.47
0.27	15.93	11.93
0.25	15.29	11.41
0.23	14.67	10.90
0.21	14.06	10.40
0.19	13.45	9.91
0.17	12.85	9.43
0.15	12.25	8.95
0.13	11.64	8.47
0.11	11.02	7.97

experimental observation that, for adsorption on rigid porous adsorbents, and provided no chemical interactions between adsorbent and adsorbate and no absorption take place, hysteresis is hardly, if ever, observed below a certain relative pressure (7), approximately 0.40 for nitrogen adsorption at its normal boiling point.

This puzzling phenomenon of hysteresis inception has long been a subject of speculation. The explanations forwarded by Cohan (7) and by Foster (8), are, to our opinion, certainly not compatible with the present treatment and are the results of erroneous ways of taking into account the influence of adsorption on capillary condensation and evaporation.

In Part IX of this series we tentatively

TABLE 2
THEORETICAL WIDTH OF THE HYSTERESIS LOOP FOR OPEN CYLINDERS, AS A FUNCTION OF THE RELATIVE PRESSURE OF CAPILLARY CONDENSATION DURING ADSORPTION

p_{ads}/p_0	$p_{ads}/p_0 - p_{des}/p_0$	p_{ads}/p_0	$p_{ads}/p_0 - p_{des}/p_0$
0.998	0.002	0.67	0.10
0.993	0.005	0.65	0.10
0.988	0.008	0.63	0.10
0.983	0.010	0.61	0.11
0.978	0.012	0.59	0.11
0.973	0.014	0.55	0.11
0.968	0.016	0.53	0.11
0.963	0.018	(0.51)	(0.11)
0.958	0.020	(0.49)	(0.11)
0.953	0.021	(0.47)	(0.11)
0.948	0.023	(0.45)	(0.11)
0.943	0.025	(0.43)	(0.11)
0.938	0.026	(0.41)	(0.10)
0.933	0.028		
0.928	0.030		
0.923	0.032		
0.918	0.034		
0.913	0.036		
0.908	0.038		
0.903	0.040		
0.89	0.04		
0.87	0.05		
0.85	0.06		
0.83	0.07		
0.81	0.07		
0.79	0.08		
0.77	0.08		
0.75	0.09		
0.73	0.09		
0.71	0.09		
0.69	0.10		

put forward a possible explanation—for very narrow pores the calculated width of the free energy barrier separating the metastable state during adsorption and the stable desorption state, whose height itself is calculated to be of the order of RT, becomes so small that crossing of this barrier must become increasingly easy. It is very questionable, however, whether the essential macroscopic concepts of capillarity applied in our treatment still hold in micropores.

A different, although also essentially macroscopic explanation, was forwarded tentatively by Flood (*9*) in a recent publication. Flood considered that according to the classical theory of capillarity, the fluid present underneath the meniscus is in a state of tension, a tension inversely proportional to the radius of curvature of the meniscus. Flood considers the possibility that for very narrow pores, and thus for very small radii of curvature, the tensile strength of the capillary-condensed fluid may be surpassed, resulting in the rupture of the capillary-condensed fluid, and therefore in capillary evaporation. According to this last hypothesis complete filling of very narrow pores would be impossible, whereas according to the views of Part IX of this series, filling would become increasingly easy.

The present situation in the theory of physical adsorption does not enable us to decide with certainty between the different alternatives, as any theory of capillary condensation based on essentially macroscopic arguments is bound to fail for very narrow pores.

IV. CLASSIFICATION OF THE HYSTERESIS LOOP OF NITROGEN SORPTION ISOTHERMS

As de Boer had already pointed out several years ago, isotherms may be classified according to the shape of the hysteresis loops into A-type, B-type, C-type, D-type, and E-type isotherms (*10*), where for each type of hysteresis loop there are only a limited number of possible pore shapes.

A-Type hysteresis loops are characterized by a steep and, often, narrow loop, as contrasted to other types of hysteresis loops. Whether a certain A-type hysteresis loop belongs to ideal tubular pores open at both ends, could in principle be decided with the aid of Table 2. For ideal tubular pores, the actual width of the hysteresis loop should coincide with the theoretical width *or be smaller when a distribution of pores is present* (which, in itself, is indicated by a decrease in steepness of the branches of the hysteresis loop). For a number of isotherms on different aluminas, as published by Lippens (*11*, *12*); on zirconias, as measured by Rijnten (*13*, *14*); and for two samples of porous glass, as published by Emmett and Cines (*15*), the width of the hysteresis loop

TABLE 3

OBSERVED WIDTH OF THE HYSTERESIS LOOP FOR A NUMBER OF ISOTHERMS AS COMPARED TO THE WIDTH THEORETICALLY TO BE EXPECTED FOR CYLINDRICAL PORES

Isotherm code	p_a/p_0	$p_a/p_0 - p_D/p_0$ Observed	$P_a/P_0 - P_D/P_0$ Calculated
By 580 [1]	0.89	0.20	0.04
	0.65	0.14	0.10
	0.51	0.05	0.11
By 750 [1]	0.89	0.07	0.04
	0.75	0.10	0.09
	0.69	0.09	0.10
BoW 450 [1]	0.95	0.027	0.022
	0.91	0.029	0.037
	0.89	0.02	0.04
MiBo 5 [1]	0.87	0.10	0.05
	0.75	0.09	0.09
	0.63	0.09	0.10
A 120 [1]	0.89	0.04	0.04
	0.79	0.06	0.08
	0.71	0.05	0.09
A 270 [1]	0.89	0.04	0.04
	0.79	0.06	0.08
	0.71	0.05	0.09
A 450 [1]	0.91	0.05	0.04
	0.83	0.06	0.07
	0.79	0.06	0.08
A 750 [1]	0.91	0.05	0.04
	0.87	0.05	0.05
	0.81	0.05	0.07
ZrO_2 280 [2]	0.65	0.15	0.10
	0.61	0.13	0.11
	0.55	0.07	0.11
ZrO_2 320 [2]	0.69	0.18	0.10
	0.59	0.11	0.11
	0.55	0.11	0.11

of the nitrogen sorption isotherm, determined at three different heights of the hysteresis loops, as compared to the width of the hysteresis loop to be expected theoretically, are given in Table 3.

The behavior theoretically to be expected for the model of open cylindrical pores is seen from the table to be followed rather closely by the isotherms on the preparations ZrO_2-450 and ZrO_2-390 by Rijnten and on Lippens' preparation BoW-450. On the other hand, for the samples of porous glass

TABLE 3 (*Continued*)

Isotherm code	p_a/p_0	$p_a/p_0 - p_D/p_0$ Observed	$P_a/P_0 - P_D/P_0$ Calculated
ZrO_2 390 [2]	0.77	0.08	0.08
	0.73	0.07	0.09
	0.69	0.06	0.10
ZrO_2 450 [2]	0.85	0.05	0.06
	0.81	0.05	0.07
	0.79	0.04	0.08
Porous glass [3]	0.73	0.20	0.09
no 4	0.67	0.14	0.10
	0.61	0.08	0.11
Porous glass [3]	0.71	0.21	0.09
no 6	0.65	0.15	0.10
	0.57	0.06	0.11
Gibbsite 204 [4]	0.95	0.44	0.022
	0.89	0.38	0.04
	0.81	0.29	0.08
Gibbsite 245 [4]	0.95	0.41	0.02
	0.89	0.38	0.04
	0.81	0.32	0.08

[1] Isotherms as given by Lippens (*11, 12*).
[2] Isotherms as given by Rijnten (*13, 14*).
[3] Isotherms of Emmett and Cines (*15*).
[4] Isotherms of de Boer, van den Heuvel, and Linsen (*16*).

by Emmett and Cines and for the preparation By-580 of Lippens, the width of the hysteresis loop at the higher relative pressure side is seen to be too large for the model of open cylinders. In accordance with this, especially the isotherms published by Emmett and Cines, show an E-type rather than an A-type behavior, suggesting the model of ink-bottle-like pores as a possibility. A certain ink-bottle character is possibly also present in the preparations ZrO_2-280 and ZrO_2-320 of Rijnten. The A preparations of Lippens also behave as ideal cylindrical pores, but the relative flatness of the branches of the hysteresis loops suggests a rather extensive distribution of pore sizes, so we would have expected the narrowing of the hysteresis loop at the low relative pressure side to be more pronounced. Possibly, some ink-bottle character is also present.

As a comparison, two isotherms published some years ago by de Boer, van den Heuvel, and Linsen (*16*), exhibiting a beautiful ink-bottle-type behavior, the preparations Gibbsite 205 and Gibbsite 245, have been included in the table. These last two examples make clear that although the other preparations mentioned may have some ink-bottle character, this character is not very outstanding in most cases, except for the samples of porous glass of Emmett and Cines.

V. Pore Distributions from the Desorption Branch of an A-Type Adsorption Isotherm

The method of calculation of pore distributions from the desorption branch of

TABLE 4
THE EQUILIBRIUM THICKNESS OF THE ADSORBED LAYER IN CYLINDRICAL PORES AS A FUNCTION OF r AND p/p_0

	r (Å)									
p/p_0	∞	128.2	67.46	44.63	33.15	26.06	21.09	17.27	14.08	11.02
0.9	14.3	18.2								
0.8	10.5	11.3	12.7							
0.7	8.57	9.01	9.55	10.5						
0.6	7.36	7.64	7.93	8.35	9.01					
0.5	6.50	6.63	6.81	7.05	7.39	7.91				
0.4	5.71	5.80	5.92	6.07	6.26	6.53	6.96			
0.3	5.01	5.09	5.17	5.26	5.37	5.52	5.74	6.10		
0.2	4.36	4.42	4.47	4.52	4.60	4.68	4.79	4.96	5.27	
0.1	3.68	3.71	3.74	3.77	3.81	3.85	3.91	3.98	4.10	4.38

a sorption isotherm in the case of an A-type hysteresis loop is completely analogous to that discussed in Part X of this series. Again the whole desorption branch is divided into a discrete number of relative pressure intervals, bounded by $x_{(k-1)}$, the higher relative pressure boundary, and x_k, the lower relative pressure boundary of the kth interval. Over each interval desorption will take place from pores having a mean radius corresponding to the mean relative pressure over the interval, while in the already empty pores there will be a change in the thickness of the adsorbed layer for each of the $k-1$ groups of pores already emptied. It was shown in Part X of this series that the pore volume of the kth group of pores with mean radius r_k, is related by the change in volume actually held by the porous system over the relative pressure interval number k, by

$$V_k = \frac{{r_k}^2}{(r_k - t_{rk,xk})^2}\left[V_k{}^e - \sum_{i=1}^{k-1} S_i(t_{ri,x(k-1)} - t_{ri,xk}) + \sum_{i=1}^{k-1}\frac{S_i}{2r_i}({t^2}_{ri,x(k-1)} - {t^2}_{ri,xk})\right] \quad (11)$$

where S_i is the surface area of the ith group of pores and $t_{ri,xk}$ is the thickness of the adsorbed layer at the relative pressure x_k in pores with a mean radius r_i.

For the actual calculation the relative pressure ranges may be taken to be equal to 0.005 for relative pressures higher than 0.90 and to be equal to 0.02 for relative pressures between 0.90 and 0.10. The mean pore radii corresponding to these relative pressure ranges are presented in Table 1. The corresponding thicknesses of the adsorbed layer for different groups of pores have to be calculated once and for all from the Eqs. (7). An abbreviated version of the resulting table is reproduced in Table 4.

The appropriate surface area for each group of pores may be calculated from the obvious relation

$$S_k = 2V_k/r_k \quad (11)$$

As was stated before, the actual calculations are too lengthy for routine desk calculations, and a high-speed electronic computing device is needed. The values of r_k and $t_{ri,xk}$ may be stored in the computer memory for later use.

VI. Results of Pore Distribution Calculations Along the Desorption Branch

The results of pore distribution calculations from the desorption branch for the isotherms discussed in Section 4, are represented in Table 5. If the model of open cylindrical pores is a reasonable one, the total cumulative surface area and pore volume should be comparable to the BET surface area (or the area calculated from the t plot), as a measure of the total surface area, and to the total pore volume as determined from the uptake of liquid nitrogen just below saturation. In general these cumulative results are of the right

TABLE 5

CUMULATIVE SURFACE AREAS AND PORE VOLUMES FOR THE MODEL OF CYLINDRICAL PORES, AS CALCULATED FROM THE DESORPTION BRANCH OF NITROGEN SORPTION ISOTHERMS BY MEANS OF EQ. (11), AS COMPARED TO THE RESULTS OF A CLASSICAL CALCULATION

Sample code[a]	p/p_0 of first deviation from linear t plot	p/p_0 of closing point of hysteresis loop	S_{BET} (m^2/g)	S_{cum} (m^2/g)	S_{cum} classical (m^2/g)	V_p (ml/g)	V_{cum} (ml/g)	V_{cum} classical (ml/g)
By 580	0.24	0.42	243	210	322	0.434	0.421	0.450
By 750	0.24	0.46	134	152	212	0.464	0.472	0.496
BoW 450	0.40	0.70	68[b]	66	83	0.479	0.478	0.489
MiBo 5	0.26	0.38	255	280	393	0.496	0.505	0.545
A 120	0.26	0.40	609	655	875	2.03	2.03	2.12
A 270	0.30	0.51	556	606	801	1.74	1.77	1.85
A 450	0.34	0.54	414	555	731	1.78	1.84	1.93
A 750	0.63	0.63	280	340	411	2.05	2.05	2.12
ZrO_2 280	0.14	0.42	240	215	322	0.252	0.238	0.266
$Zr{\cdot}O_2$ 320	0.19	0.45	180	170	252	0.201	0.190	0.216
ZrO_2 390	0.36	0.53	100	103	140	0.183	0.194	0.205
ZrO· 450	0.64	0.64	64	64	85	0.190	0.190	0.199
Por·glass 4	0.38	0.42	25.1	22	32	0.0305	0.0290	0.0315
Por·glass 6	0.44	0.50	20.6	16	26	0.0227	0.0193	0.0235

[a] For indication of authors, see Table 3.

[b] Surface area present in wide pores, as determined from the t plot.

order of magnitude and compare favorably to the results of cumulative calculations making use of the classical Kelvin equation and the familiar B.J.H. method, as presented in the same table.

For ideal cylindrical pores, the cumulative distribution curves from the adsorption branch as calculated according to the method of Part X (*20*) should coincide with the corresponding curves as calculated from the *desorption* branch according to the method of the present article. This is a rather severe test of both the proposed method of calculation and of the pore model. The shapes of the hysteresis loops of the isotherms used for the calculations, are discussed elsewhere (*12*, *13*). From these discussions, in concordance with the conclusions to be drawn from Table 3, it appears that the isotherms A 120 and BoW 450 of Lippens (*12*) and ZrO_2-390 and ZrO_2-450 of Rijnten (*13*, *14*) may be taken as reasonably good examples of A-type hysteresis loops. In Fig. 1a–d we have compared the cumulative calculation along the adsorption branch to that from the desorption branch for the samples just mentioned. It is seen that the consistency between both methods of calculation is rather good, despite the approximative character of the cylindrical pore shape even for these samples.

On the other hand the samples of porous glass, as taken from the publication of Emmett and Cines, show an E-type hysteresis loop, indicating ink-bottle-shape pores. The corresponding cumulative calculations, as shown in Fig. 1e, f, are not consistent, not only so in the narrow-pore region but also in the wide-pore region. This is what would be expected for ink-bottle-shape pores.

As we pointed out before, the desorption branch is the thermodynamically stable branch only for open cylinders and for cylinders closed at one side (*17*). Type II ink bottles, viz., cylinders fitted with narrow restrictions, behave, during adsorption, as closed cylinders and the adsorption branch is the thermodynamically stable branch. In this case the formulas and pore radii as given in the present paper have to be applied to the adsorption branch. The application of this procedure does not, of course, permit a comparison between the results of the adsorption branch and of the desorption branch. The only possibility is to

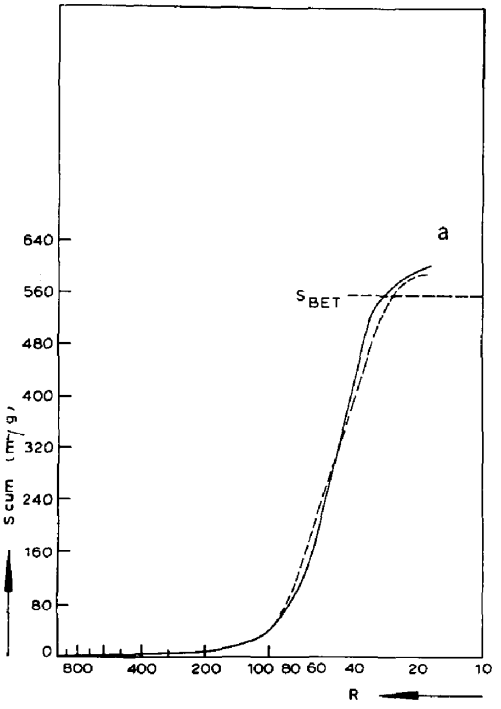

FIG. 1a

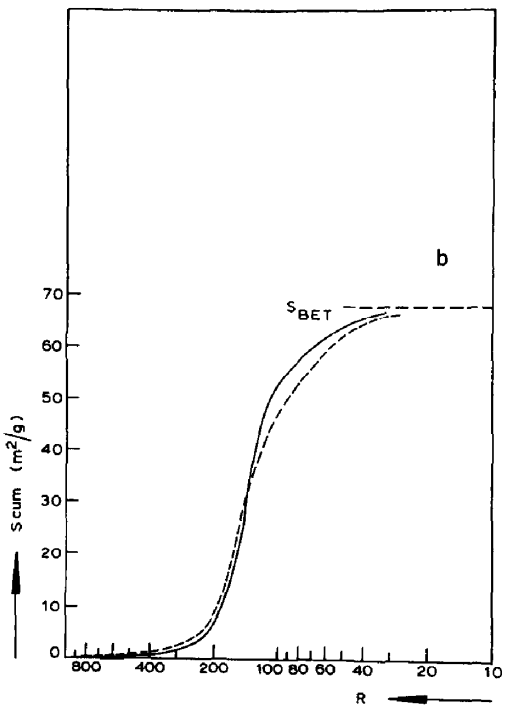

FIG. 1b

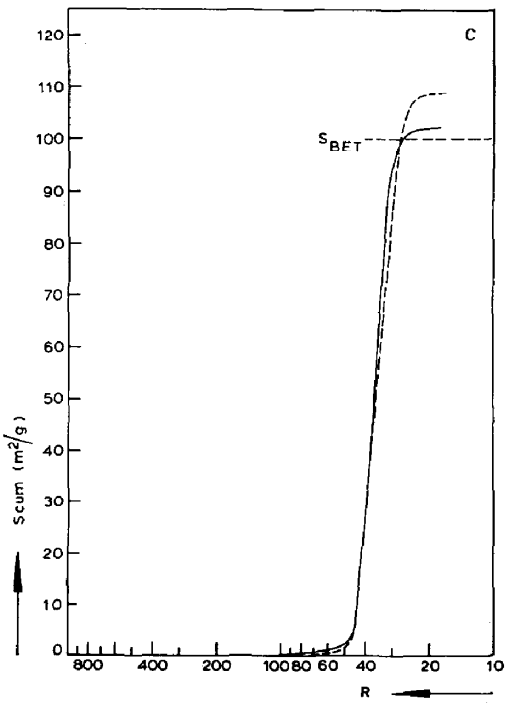

FIG. 1c

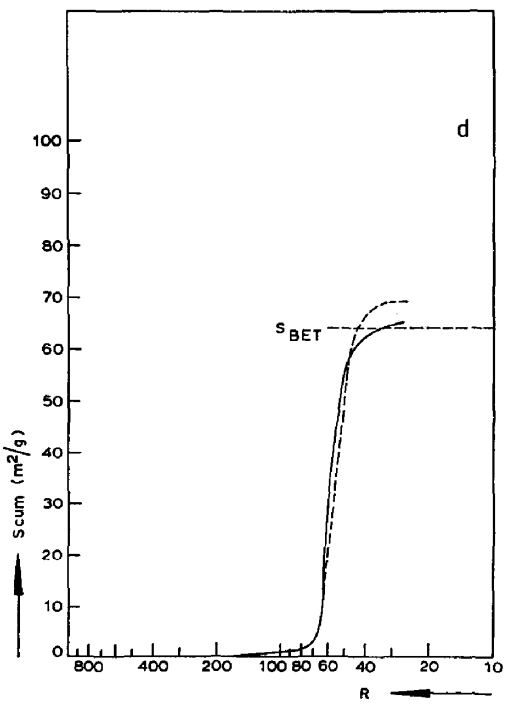

FIG. 1d

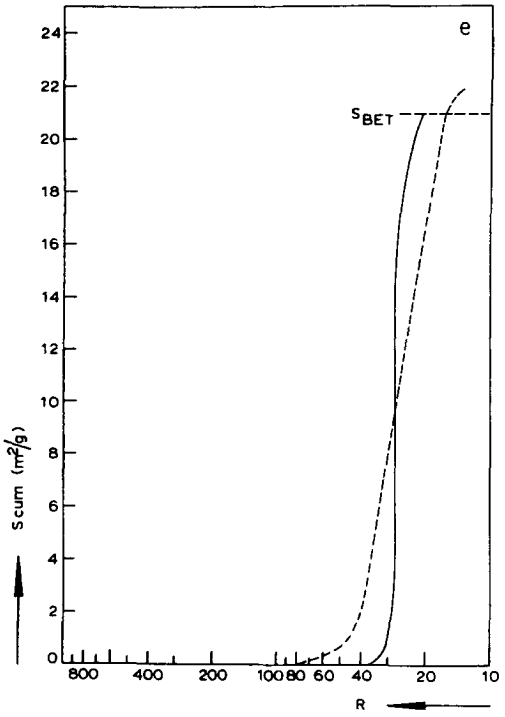

FIG. 1e

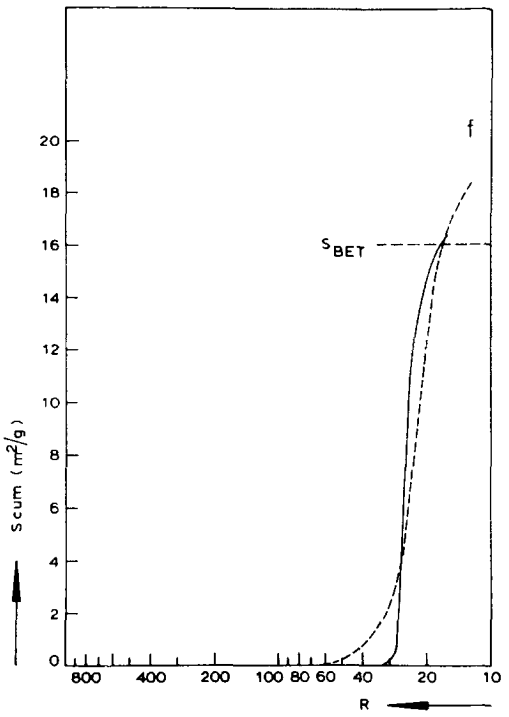

FIG. 1f

FIG. 1. A comparison between cumulative surface area distribution curves, as calculated along the adsorption branch and the desorption branch: full lines, desorption branch; dashed lines, adsorption branch; (a) sample A 120; (b) BoW 450; (c) ZrO_2 390; (d) ZrO_2 450; (e) porous glass no 4; (f) porous glass no 6.

compare the total pore volume and surface area to the total cumulative values. In general the assumption of Type II ink bottles leads to a considerable lowering of cumulative areas. As an illustration some results of such a calculation are gathered in Table 6. Concordance is not especially good for the isotherms used for the calculations of the present article.

TABLE 6

CUMULATIVE SURFACE AREAS CALCULATED FROM THE ADSORPTION BRANCH OF THE NITROGEN SORPTION ISOTHERMS, MAKING USE OF THE METHOD OF CALCULATION PROPOSED IN THE PRESENT ARTICLE

	Preparation code[a]					
	A120	A270	A450	A750	By580	Porous glass no 4
S_{cum} (m^2/g)	570	505	426	240	180	15
S_{BET} (m^2/g)	609	556	414	280	243	25.5

[a] For authors of isotherms see legend to Table 3.

VII. DISCUSSION

It has been shown that, in a number of cases, the application of corrected Kelvin equations leads to consistency between the results obtained from the adsorption branch and from the desorption branch, respectively, consistency which is hardly ever found when the uncorrected Kelvin equations are applied. On the other hand, the calculations of pore distributions are based on a number of simplifications and idealizations, one of which is the assumption of highly idealized pore models. Ideal pore shapes will hardly ever be encountered in porous materials found in practice. This may not detract us from the fact that the use of corrected Kelvin equations of the form discussed in the last four articles of this series, in general leads to reasonable cumulative results, indicating that such refinements are not of mere academic interest. Meanwhile, the significance of certain dis-

crepancies between cumulative surface areas and, for example, BET surface areas should not be overstressed, as a complete concordance is not to be expected in view of the inherent approximate character of every method of pore distribution calculations.

Moreover, it is not pretended that the results of cumulative calculations lead to certainty with regard to the shape of the pores present. A careful study of the shape of the hysteresis loop, of the characteristics of the t plot of the adsorption branch of a nitrogen sorption isotherm (*18*), together with the results of cumulative calculations along the adsorption and the desorption branch using different pore models may give valuable information about the most probable pore shape to be expected, provided the radius of the pores is not very small.

This information may be combined with information from other sources such as electron microscopy and crystallographic information (*19*), yielding the most probable pore model. It is very difficult, except in exceptional cases, to evaluate the pore shape with certainty from sorption data alone. Also the mode of preparation of the porous material may yield some information with respect to the expected pore shape. Tubular or spheroidal pores may be expected in cases where the porous material is compounded from randomly oriented small crystallites or small spherical particles, whereas the lamilar structure of, e.g., graphitic oxide suggests rather the model of slit-shaped pores. When tubular or spheroidal pores are expected, the methods developed in this series for the calculation of pore distribution may be applied. For tubular pores the results from the adsorption branch and from the desorption branch should be reasonably consistent, whereas for ink-bottle-like pores such a consistency should be absent. In this last case the results obtained from the adsorption branch should be preferred. If the shape and the width of the hysteresis loop, together with the available crystallographic information, suggests rather slit-shaped pores, the model of slits should be applied. For this model, however, the same corrections as were applied to the cylindrical and spheroidal model, should be taken into account. Explicit formulas for this last model will be derived in the next paper of this series.

References

1. Broekhoff, J. C. P., and de Boer, J. H., *J. Catalysis* **9**, 8 (1967).
2. Broekhoff, J. C. P., and de Boer, J. H., *J. Catalysis* **10**, 366 (1968) (Part XII) (preceeding paper).
3. Dubinin, M. M., *Pure Appl. Chem.* **10** (No. 4), 309 (1963).
4. Harkins, W. D., and Jura, D., *J. Am. Chem. Soc.* **66**, 1362 (1944).
5. Derjaguin, B. V., *Proc. Intern. Conf. Surface Activity, 2nd, London*, 1957, p. 153. Butterworth, London, 1958.
6. See de Boer, J. H. The shape of capillaries, *in* "The Structure and Properties of Porous Materials" (D. H. Everett and F. S. Stone, eds.) (Butterworth, London, 1958).
7. Cohan, L. H., *J. Am. Chem. Soc.* **60**, 433 (1938).
8. Foster, A. G., *J. Chem. Soc.*, p. 1806 (1952).
9. Flood, E. A., *in* "The Solid–Gas Interface" (E. A. Flood, ed.), Vol. I, p. 58. (Dekker, New York, 1967).
10. de Boer, J. H., The shape of capillaries, *in* "The Structure and Properties of Porous Materials" (D. H. Everett and F. S. Stone, eds.) (Butterworth, London, 1958).
11. Lippens, B. C., Doctoral Thesis, Delft, The Netherlands, 1961, p. 128.
12. Lippens, B. C., and de Boer, J. H., *J. Catalysis* **3**, 38 (1964).
13. de Boer, J. H., *Proc. British Ceramic Society* **5**, 5 (1965).
14. Rijnten, H. Th., Doctoral Thesis, Delft, The Netherlands, to be published.
15. Emmett, P. H., and Cines, M., *J. Phys. Colloid Chem.* **51**, 1260 (1947).
16. de Boer, J. H., van den Heuvel, A., and Linsen, B. G., *J. Catalysis* **3**, 268 (1964).
17. Broekhoff, J. C. P., and de Boer, J. H., *J. Catalysis* **10**, 153 (1968). (Part XI).
18. Lippens, B. C., and de Boer, J. H., *J. Catalysis* **4**, 319 (1965).
19. de Boer, J. H., Fortuin, J. M. H., and Steggerda, J. J., *Proc. Koninkl. Ned. Akad. Wetenschappen, B***57**, 434 (1954).
20. Broekhoff, J. C. P., and de Boer, J. H., *J. Catalysis* **9**, 15 (1967) (Part X).